

Cusp or core? Revisiting the globular cluster timing problem in Fornax

Noah Meadows¹, Julio F. Navarro¹, Isabel Santos-Santos¹, Alejandro Benítez-Llambay², Carlos Frenk²

¹*Department of Physics and Astronomy, University of Victoria, Victoria, BC V8P 5C2, Canada*

²*Institute for Computational Cosmology, Durham University, South Road, Durham DH1 3LE, United Kingdom*

1 September 2022

ABSTRACT

We use N-body simulations to revisit the globular cluster (GC) “timing problem” in the Fornax dwarf spheroidal (dSph). In agreement with earlier work, we find that, due to dynamical friction, GCs sink to the center of dark matter halos with a cuspy inner density profile but “stall” at roughly 1/3 of the core radius (r_{core}) in halos with constant-density cores. The timescales to sink or stall depend strongly on the mass of the GC and on the initial orbital radius, but are essentially the same for either cuspy (NFW) or cored halos normalized to have the same total mass within r_{core} . Arguing against a cusp on the basis that GCs have not sunk to the center is thus no different from arguing against a core, unless all clusters are today at $\sim (1/3)r_{\text{core}}$. This would imply a core radius exceeding ~ 3 kpc, much larger than seems plausible in any core-formation scenario. (The average projected distance of Fornax GCs is $\langle R_{\text{GC,Fnx}} \rangle \sim 1$ kpc and its effective radius is ~ 700 pc.) A simpler explanation is that Fornax GCs have only been modestly affected by dynamical friction, as expected if clusters started orbiting at initial radii of order ~ 1 – 2 kpc, just outside Fornax’s present-day half-light radius but well within the tidal radius imprinted by Galactic tides. This is not entirely unexpected. Fornax GCs are significantly older and more metal-poor than most Fornax stars, and such populations in dSphs tend to be more spatially extended than their younger and more metal-rich counterparts. Contrary to some earlier claims, our simulations further suggest that GCs do not truly “stall” at $\sim 0.3r_{\text{core}}$, but rather continue decaying toward the center, albeit at reduced rates. We conclude that dismissing the presence of a cusp in Fornax based on the spatial distribution of its GC population is unwarranted.

Key words: galaxies: clusters: general – galaxies: haloes – galaxies: dwarf

1 INTRODUCTION

The globular cluster (GC) system of the Fornax dwarf spheroidal (dSph) is often cited as evidence for the presence of a constant-density core in the dark matter halo density profile. The issue has been addressed repeatedly in the literature, starting with the early work of [Hernandez & Gilmore \(1998\)](#), who were among the first to describe how the spatial distribution of globular clusters may be used to gain insight into the dark matter density distribution in dSphs. This elaborated on the earlier work of [Tremaine \(1976\)](#), who puzzled about the lack of a central stellar “nucleus” in Fornax, expected from the orbital decay and subsequent fusion of its GCs. Indeed, the 5 GCs in Fornax are widely spread

through the galaxy, with an average projected radius¹ of $\langle R_{\text{GC,Fnx}} \rangle \sim 1$ kpc ([Mackey & Gilmore 2003](#)), despite the fact that their orbital decay timescales, inferred at the time from simple analytical dynamical friction estimates ([Chandrasekhar 1943](#)), were substantially shorter than their ages.

This puzzle is widely referred to as the Fornax “GC timing problem” and has elicited the proposal of a number of possible solutions, ranging from the “dynamical stirring” of GC orbits by Galactic tides or massive black holes ([Oh et al. 2000](#)), to more straightforward options, such as assuming that GCs in Fornax started decaying from initial radii

¹ For comparison, Fornax’s effective radius is $R_{\text{eff,Fnx}} \sim 700$ pc ([Irwinn & Hatzidimitriou 1995](#)).

somewhat larger than where they are currently at (Angus & Diaferio 2009; Boldrini et al. 2019).

An alternative solution was proposed by Goerdt et al. (2006), who reported some of the first fully self-consistent N-body simulations of the problem. These authors found that analytical predictions for dynamical friction-induced orbital decay fail in the case of halos with constant-density cores. Instead of continually decaying, GCs “stall” once they are well inside the core, at a radius that is roughly independent of GC mass. In cuspy halos, such as the Navarro-Frenk-White profiles of cold dark matter (CDM) halos (NFW; Navarro et al. 1996b, 1997), GCs do not stall but rather sink until they reach either the center or a radius where the enclosed dark mass is comparable to that of the cluster (Goerdt et al. 2010).

The “stalling radius” result has been reproduced in subsequent work (see; e.g., Read et al. 2006; Inoue 2009; Petts et al. 2015; Kaur & Sridhar 2018), and has become an often cited argument for the presence of a core in Fornax: if GCs “stall at the core radius”, as is often claimed, then for $\langle R_{\text{GC,Fnx}} \rangle \approx r_{\text{core}} \sim 1$ kpc the timing problem would be solved.

A core radius of that size would be comparable to Fornax’s effective radius, as expected if cores are carved out of cuspy, NFW halos by baryonic inflows/outflows during the formation of the galaxy (see; e.g., Navarro et al. 1996a; Pontzen & Governato 2012; Di Cintio et al. 2014, and references therein). It would also be commensurate with the core size expected for Fornax in models where cores are produced by “self-interactions” between dark matter particles (Spergel & Steinhardt 2000; Rocha et al. 2013; Kaplinghat et al. 2016), at least for self-interacting cross sections in the preferred range of 0.1-1 cm²/g. These coincidences have helped galvanize support for the “core” solution to the Fornax GC timing problem.

One problem with this solution is that the stalling radius is actually well inside the core²; i.e., $r_{\text{stall}} \sim 0.3 r_{\text{core}}$. Taken at face value, this would imply that a core radius as large as ~ 3 kpc would be needed to solve the timing problem, a value that seems, in principle, much larger than can be reasonably accommodated by current core-formation models.

One reason why cores remain a viable solution is that subsequent simulation work uncovered a rather puzzling phenomenon that affects clusters that reach the inner regions of the core. In the simulations reported by Cole et al. (2012), clusters well inside the core tend to *gain* orbital energy, and are pushed out by “dynamical buoyancy”, a mechanism whose detailed origin remains unclear but which apparently counteracts dynamical friction in the innermost regions. The combination of friction and buoyancy could, in principle, lead to a stationary “shell-like” distribution of globulars near the core radius, where the two effects would presumably cancel out. Although appealing, this result relies on a mechanism that is still poorly understood and that ur-

gently needs theoretical underpinning and independent numerical confirmation.

We address some of these issues here using a series of N-body simulations of the decay of GCs in cuspy or cored halos. We focus on the difference in the timescales needed for clusters to “sink” (i.e., to reach the center, in the case of cusps), or to “stall” (in the case of cores). We also follow the long-term evolution of several clusters after they stall, in order to learn about the possible effects of dynamical buoyancy on these systems.

This paper is organized as follows. Sec. 2 describes our numerical setup, while our main results are presented in Sec. 3. We conclude with a discussion of the applicability of these results to Fornax and to the ongoing cusp vs core debate in Sec. 4.

2 NUMERICAL SIMULATIONS

The simulations follow the evolution of a GC (represented by a softened point mass) in two spherical N-body halo models. The first model is a cuspy, NFW halo (hereafter, “NFW”) with parameters consistent with those expected in a Planck-normalized Λ CDM cosmology (Ludlow et al. 2016). The second model is a non-singular isothermal sphere (hereafter, “ISO”) normalized to have the same mass as the NFW profile within its core radius.

2.1 Halo models

The cuspy halo model follows an NFW profile,

$$\rho(r) = \frac{\rho_s}{(r/r_s)(1+r/r_s)^2}, \quad (1)$$

and is fully specified by two parameters; e.g., a scale density, ρ_s , and a scale radius, r_s , or, alternatively, a maximum circular velocity, V_{max} and the radius at which it is achieved, r_{max} . The two radial scales are related by $r_{\text{max}} = 2.16 r_s$.

The cored halo is modeled as a non-singular isothermal sphere (see; e.g., Binney & Tremaine 1987, p.228). Although there is no simple algebraic formula to describe this model, it is also fully specified by two parameters, usually expressed as the central density, ρ_0 , and the core radius, r_{core} .

The models are assumed to have isotropic velocity distributions and are normalized to have the same enclosed mass within the deprojected (3D) half-light radius of Fornax, $M(< 1 \text{ kpc}) = 10^8 M_{\odot}$, inferred from observations of the line-of-sight velocity dispersion and projected light profile of Fornax (Walker et al. 2009; Wolf et al. 2010). This is widely agreed to be the most robust dynamical mass estimate available for this system (see the discussion of Fig. 1 in Fattahi et al. 2016, and references therein).

Fig. 1 contrasts the density, $\rho(r)$, circular velocity, $V_c(r)$, enclosed mass, $M(r)$, and radial velocity dispersion, $\sigma_r(r)$, profiles of the two models. The NFW profile has $r_s = 2.11$ kpc and $\rho(r_s) = (\rho_s/4) = 3 \times 10^6 M_{\odot}/\text{kpc}^3$. This corresponds to a “virial”³ mass $M_{200} = 2.7 \times 10^9 M_{\odot}$ and concentration $c =$

² We shall hereafter define the core radius, r_{core} , as the (3D) radius where the dark matter density drops by a factor of two from its central value. Since this convention is not always followed, care is needed when comparing quantitative results from different authors.

³ Virial quantities are conventionally defined as those measured at a radius where the mean enclosed density equals 200× the critical density for closure, and are identified with a “200” subscript.

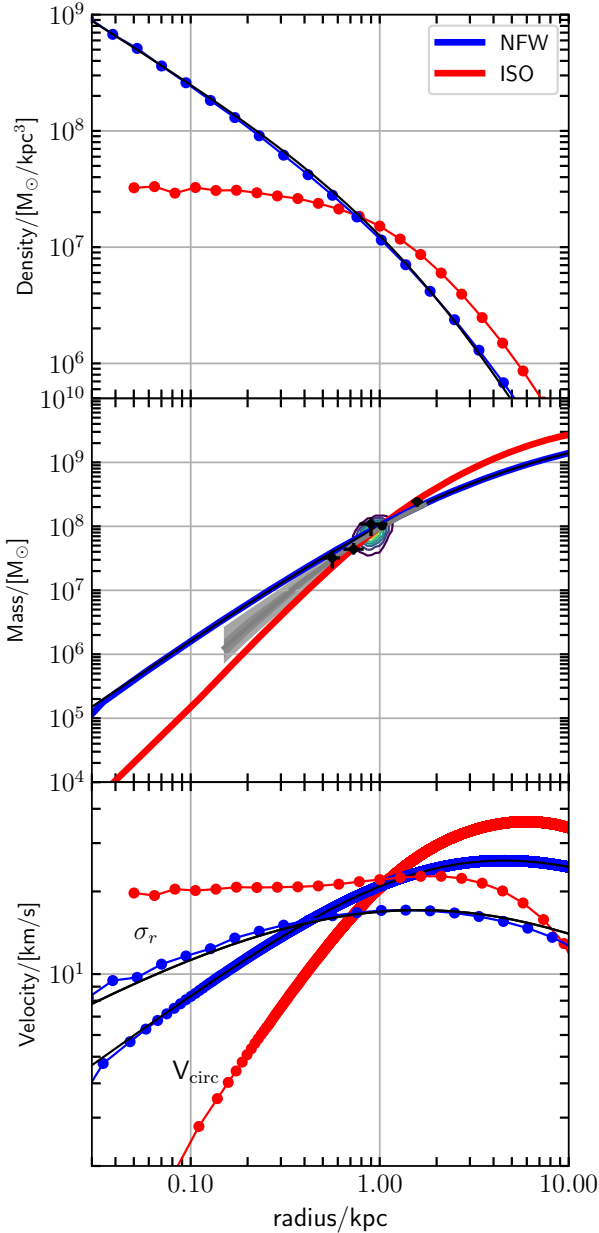


Figure 1. Density (top), enclosed mass (middle) and circular velocity/radial velocity dispersion (bottom) profiles of the halo models used in this study. The profiles (shown with circles/thick curves) correspond to the 16M-particle N-body realization of each model, and are plotted after the halo has been run for ~ 4 Gyr to allow it to relax to equilibrium. Blue corresponds to the cuspy NFW halo, and red to the non-singular isothermal (cored) halo. The analytic NFW profile is shown with thin black lines. The contours in the middle panel are constraints on the enclosed mass within ~ 1 kpc, derived from the stellar velocity dispersion and density profiles (see Fattahi et al. 2016, for details). In the same panel, crosses indicate the estimates of Walker & Peñarrubia (2011) and Amorisco et al. (2013). The grey shaded band corresponds to the recent kinematic analysis of Read et al. (2019). All of these estimates coincide at $r \sim 1$ kpc.

$r_{200}/r_s = 14$. The isothermal profile has $\rho_0 = 3 \times 10^7 M_{\odot}/\text{kpc}^3$ and $r_{\text{core}} = 1$ kpc.

The contours in the middle panel of Fig. 1 indicate the constraints derived by Fattahi et al. (2016) on $M(< 1 \text{ kpc})$. For comparison, we also indicate with crosses the constraints at various radii from Walker & Peñarrubia (2011) and Amorisco et al. (2013). The grey shaded band corresponds to the results of the recent kinematic analysis of Fornax’s stellar component of Read et al. (2019). Note how all of these estimates concur at $r \sim 1$ kpc to a mass close to what is assumed in our models.

For reference, the circular orbit timescale is $t_{\text{circ}} \approx 3 \times 10^8$ yr at $r = 1$ kpc for both models; at $r = 0.1$ kpc, $t_{\text{circ}} = 8 \times 10^7$ yr for the NFW case, and $t_{\text{circ}} = 2.2 \times 10^8$ yr for the cored halo.

2.2 GC models

GCs are modeled as single softened point masses. Three different masses were chosen in our runs: a fiducial value of $M_{\text{GC}} = 3 \times 10^5 M_{\odot}$, similar to Fornax GC3 (NGC 1049), the most massive cluster orbiting Fornax (Mackey & Gilmore 2003). We also explored models with $M_{\text{GC}} = 10^5 M_{\odot}$, comparable to GC2, GC4 and GC5. The other GC in Fornax has much lower mass (GC1, $3.7 \times 10^4 M_{\odot}$). Recall that dynamical friction timescale inversely with mass. In the absence of other complicating factors, and in the regime where the GC mass is small compared to that enclosed within its orbit, the orbital decay of different clusters should be similar, once their times are inversely scaled by cluster mass. We assume that GC masses remain constant during the evolution. This neglects possible mass losses due to internal collisional processes within the cluster. Including this effect would result in even longer orbital decay timescales than the ones reported here, so our results may be regarded as conservative from that point of view.

2.3 N-body models

Equilibrium N-body models with 1.6 and 16 million particles are generated for each halo using the software package **Zeno**⁴ developed by Josh Barnes at the University of Hawaii. The N-body models are truncated with an exponential taper in the outer regions, but this should be of no consequence for our analysis.

The simulations were run with the publicly available **Gadget2** code (Springel 2005), with standard numerical integration parameters. Pairwise interactions between N-body particles are softened with a Plummer-equivalent softening length of $\epsilon_p = 66.4$ and 210 pc, for the 16M and 1.6M particle halos, respectively. The halo particle mass is $1.78 \times 10^2 M_{\odot}$ (cusp) and $1.99 \times 10^2 M_{\odot}$ (core) for the 16M particle realizations. Particle masses are $10\times$ larger for the 1.6M-particle halos.

Each halo model is run for ~ 4 Gyr in isolation to allow them to equilibrate and fully relax before introducing the GC. The profiles shown in Fig. 1 are measured at the end of these equilibration runs. Careful centering is required to

⁴ <http://www.ifa.hawaii.edu/faculty/barnes/zeno/>

obtain robust results; we use in our analysis the center (position and velocity) defined by the potential-weighted center of mass of all halo particles.

GC particles are softened with $\epsilon_{p,GC} = 13$ pc and are introduced at the end of the equilibration period. They are placed at various radii (typically $r_{init} = 0.5, 1,$ and 2 kpc) on circular orbits with random orientations. Their radial evolution is then monitored as a function of time. Most of the runs reported here correspond to the 1.6M model; a representative sample of those have been repeated with the 16M-particle model, with indistinguishable results. We have also repeated several runs varying $\epsilon_{p,GC}$. No significant variations were seen in the GC orbital evolution for values of $\epsilon_{p,GC}$ smaller than adopted for our runs, although substantially longer dynamical friction decay times were seen for (unrealistically) large values of $\epsilon_{p,GC}$. For $\epsilon_{p,GC} \sim 100$ pc, for example, GCs take roughly twice as long to decay than for our fiducial value of 13 pc.

3 RESULTS

3.1 Orbital decay timescales

The time evolution of the fiducial mass GC ($M_{GC} = 3 \times 10^5 M_{\odot}$, similar to the most massive Fornax GC, NGC 1049) is shown in the top panel of Fig. 2. The figure shows the evolution of three different runs per halo, each with different starting radii, $r_{init} = 2, 1,$ and 0.5 kpc. Curves for the latter two have been shifted horizontally so that they coincide in radius and time, at the beginning, with the $r_{init} = 2$ kpc case. All three curves are essentially indistinguishable from each other. This highlights the fact that the GC evolution is independent of starting radius, as expected if orbits remain roughly circular throughout the evolution.

This figure illustrates a few interesting points. One is that, if NGC 1049 had formed at 2 kpc from the center, then it would only have decayed to a distance of ~ 1 kpc after a Hubble time. The orbital decay accelerates once the cluster reaches 1 kpc, and the cluster quickly sinks to the center in the case of the cusp, or “stalls” at $r_{stall} \sim 0.3 r_{core} = 300$ pc in the case of the core.

This behaviour is consistent with earlier work (see; e.g., Goerdt et al. 2006; Read et al. 2006; Cole et al. 2012): GCs always stall at $\sim 0.3 r_{core}$, when the core radius is defined as that where the density drops to half its central value.

Interestingly, the time the cluster takes to either sink or stall is approximately the same, ~ 18 Gyrs (~ 4 Gyrs since the cluster reached 1 kpc) in both cases. In other words, *dynamical friction timescales in cored or cuspy halos are essentially indistinguishable* for halos normalized as in Fig. 1. The difference is in the final radius reached by the cluster: ~ 300 pc in the case of the core, or the center in the case of the cusp.

The middle panel of Fig. 2 confirms this conclusion for the case of a cluster $5 \times$ more massive, $M_{GC} = 1.5 \times 10^6 M_{\odot}$. The evolution of this cluster is exactly analogous to that of its less massive counterpart shown in the top panel. The timescales to sink or stall are still roughly the same for cusp or core, albeit $5 \times$ shorter than in the former case, just as expected from the mass ratio between those clusters.

Conversely, for clusters less massive than our fiducial

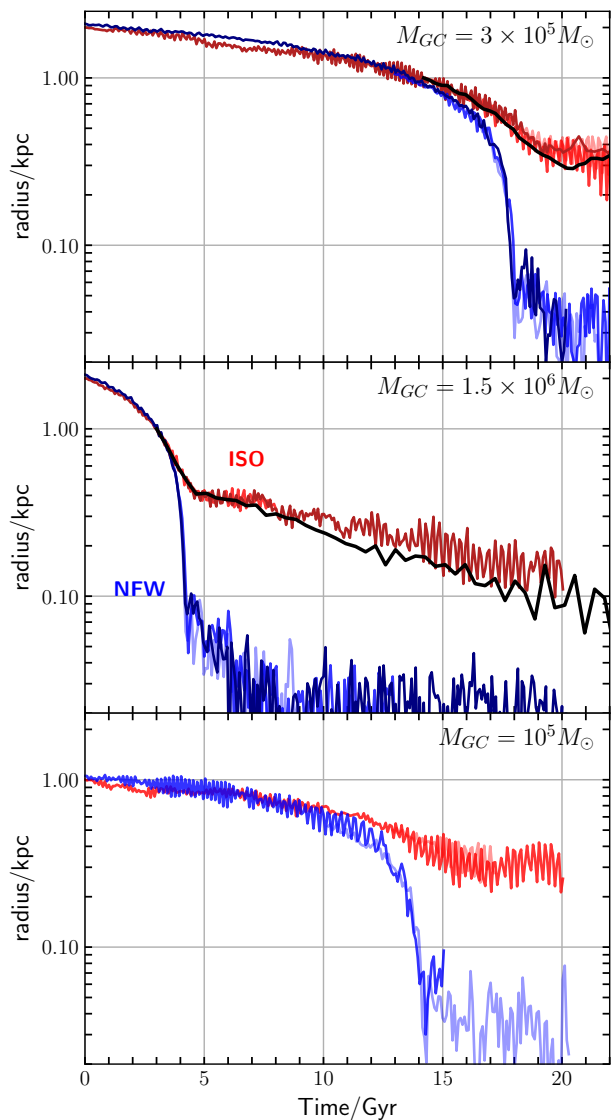


Figure 2. Evolution of the radial distance of a $M_{GC} = 3 \times 10^5 M_{\odot}$ (top), $M_{GC} = 1.5 \times 10^6 M_{\odot}$ (middle), and $M_{GC} = 10^5 M_{\odot}$ (bottom) globular cluster. The evolution is followed for roughly 20 Gyrs. The cuspy, NFW halo case is shown in blue; the core case in red. (The curves in black correspond to the 16M-particle halo model.) Different hues correspond to independent runs with different initial radii, $r_{init} = 2, 1,$ and 0.5 kpc, respectively, and are shown after shifting their time origin so that their starting radii coincide. The near perfect overlap between different curves shows that the numerical results are independent of starting radii, as expected if clusters remain on a nearly circular orbits as they decay. Clusters either sink to the center (cusp) or stall (core), but do so on similar timescales. The top panel corresponds to a cluster with mass comparable to the most massive GC in Fornax (GC3/NGC 1049). Its orbit decays from 2 to 1 kpc in ~ 13 Gyr, before stalling (core) or sinking (cusp) after ~ 18 Gyr. The middle panel represents a cluster $5 \times$ more massive than NGC 1049. The bottom panel corresponds to a mass comparable to GC2, GC4 and GC5.

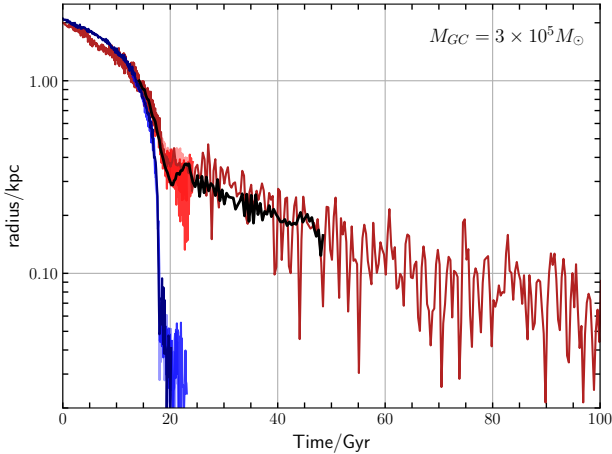


Figure 3. As Fig. 2, but following the evolution for $t = 100$ Gyr. Note that the GC keeps decaying inside the core, but on a $\sim 5\times$ longer timescale than in Fig. 2, as expected given the mass ratio between the clusters.

mass, the decay timescales are substantially longer. The results for $M_{GC} = 10^5 M_{\odot}$ (comparable to Fornax GC2, GC4, and GC5) are shown in the bottom panel of Fig. 2, and show that clusters with $r_{\text{init}} = 1$ kpc take more than 13 Gyrs to either sink or stall. This is as expected from the fiducial ($3 \times 10^5 M_{\odot}$) mass case, which takes ~ 4 Gyrs to sink or stall from a radius of 1 kpc. Placed at $r_{\text{init}} > 1$ kpc, GC2, GC4, and GC5 would have barely evolved over 13 Gyr. Again, the evolution shown in the three panels of Fig. 2 are all analogous and consistent with each other, once times are scaled by the mass of a cluster and comparisons are made for the same starting radius.

3.2 Long-term evolution

The middle panel of Fig. 2 follows the evolution of the most massive cluster in our series for ~ 20 Gyr, quite a long period of time after its initial stall/sink. This allows us to probe the long-term evolution of the clusters once they reach the inner regions of the halo. In the case of the cusp, once the cluster sinks to the center it stays there. In the case of the core, after its initial stall the cluster keeps losing energy and slowly drops deeper inside the core. At the end of the simulation the cluster has reached a radius of ~ 200 pc, roughly where the halo enclosed mass is comparable to its own (see Fig. 1). Note that we find the same result for the 1.6M and 16M-particle halos, so the long-term sinking behaviour seems robust.

This long-term evolution is not unique to this massive cluster. The fiducial mass GC also keeps losing energy after its initial stall, as shown in Fig. 3. The main difference is that this long-term trend takes, as expected, $5\times$ longer, and is therefore only noticeable in simulations that follow the evolution for roughly ~ 100 Gyr. Indeed, after that time the cluster has shrunk its orbit to roughly 100 pc, which is about the radius where the enclosed mass of the halo matches that of the cluster.

These results seem to disagree with those of Cole et al.

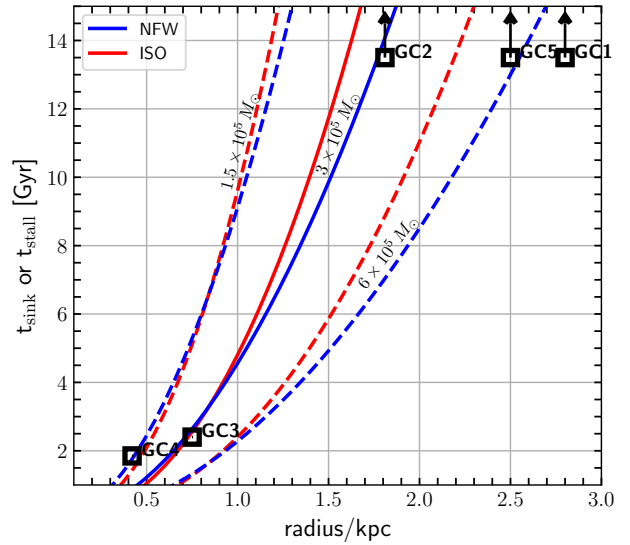


Figure 4. Time to stall (core, in red) or sink (cusp, in blue) as a function of GC mass and initial radius. Note that, at given radius and mass, the timescales are similar for cuspy and cored halos normalized to the same mass within $r_{\text{core}} = 1$ kpc (Fig. 1). As expected, timescales scale inversely with mass, and are strongly dependent on initial radius. Fornax GCs are placed on this figure at radii equal to $\sqrt{3}\times$ the present-day projected distance, and at a location consistent with its mass. Note that only GC3 and GC4 are expected to evolve significantly due to dynamical friction over the next few Gyrs. See text for a full discussion

(2012), who report that clusters that drop deep into the core of a halo are pushed out by a mechanism they call “dynamical buoyancy”. This effect was only seen in the case of their “large core” (LC) halo, which is actually quite similar to the ISO halo we adopt here. Indeed, the LC halo has $r_{\text{core}} \sim 1.2$ kpc (only 20% larger than ISO’s) and $\rho_0 \sim 4 \times 10^7 M_{\odot}/\text{kpc}^3$ (about 33% larger than ISO’s). The main difference is that the LC density profile steepens faster than ISO’s: at r_{core} the logarithmic slope is $d \log \rho / d \log r = -1.8$ for LC and -1.1 for ISO. This difference seems, at face value, too small to explain why we do not see “dynamical buoyancy” in our runs. At this point it is unclear what the origin of the discrepancy might be, but it is something that we plan to investigate in future work.

4 DISCUSSION AND CONCLUSIONS

In agreement with earlier work, our simulations indicate that the GC population of Fornax is expected to evolve continuously due to dynamical friction. For the halo models considered here (Sec. 2.1), our results are summarized in Fig. 4, where we plot the time it would take for clusters of various masses to sink (NFW, blue) or stall (ISO, red). These times are computed by fitting the results of our simulations with simple power laws and, therefore, in a strict sense, apply only to clusters in circular orbits. However, these times are not expected to differ much from those for clusters in non-circular orbits with comparable average radii (Angus & Diaferio 2009).

We compare these results with Fornax GCs (shown with open squares), taking into account the masses of individual clusters and assuming that they are at radii $\sqrt{3} \times$ their current projected distance. Our results indicate that both GC3 and GC4 (the two closest to the center, with projected distances of 0.43 and 0.24 kpc, respectively; Mackey & Gilmore 2003) should either sink or stall over the next few Gyr⁵.

On the other hand, GC1, GC2, and GC5 are either too far, or have too little mass, to decay significantly, even over a timespan as long as the next 10-15 Gyr. It is thus highly unlikely that all clusters are today at a common radius dictated by dynamical friction effects.

Changes to the spatial distribution of the Fornax GC population over a Hubble time are thus likely restricted to only two clusters; GC3 and GC4. If Fornax has a core and these two clusters have “stalled” then they must be orbiting at about the same radius, roughly $r_{\text{stall}} \sim 600$ pc from the center; their average 3D distance from the center. This implies $r_{\text{core}} \sim 2$ kpc (i.e., at least twice as large as its 3D stellar half-mass radius; recall that $r_{\text{stall}} \approx 0.3 r_{\text{core}}$).

A radius this large seems difficult to accommodate in either of the two leading scenarios for core creation; i.e., baryonic outflow-induced cores, or dark matter self-interactions. Indeed, if cores are carved out of CDM halos through stellar feedback, then it would be difficult to explain a core size at least twice as large as the half-light radius of the galaxy (Pontzen & Governato 2014; Oman et al. 2016).

On the other hand, if cores are due to self-interacting dark matter, these would be expected to be of sub-kpc scale in galaxies as small as Fornax, even for extreme values of the cross section. Elbert et al. (2015), for example, report sub-kpc core radii⁶ even for halos substantially more massive than Fornax, and for all values of the cross section in the plausible range of 0.1-1 cm²/g (the same is true even for larger cross sections; see, e.g., Sameie et al. 2019).

If, on the other hand, Fornax has a cusp, then GC3 and GC4 must be on their way to sinking to the center, having formed/started their decay after forming ~ 10 Gyr ago at $r_{\text{init}} \sim 1.6$ kpc (GC3) and $r_{\text{init}} \sim 1$ (GC4), as in the earlier analytical study of Angus & Diaferio (2009). These initial radii are quite plausible, as they lie well within the inferred tidal radius of Fornax imposed by the Galactic tides, which is estimated to be of order 1.8-2.8 kpc (Cole et al. 2012).

It could be argued that, because the sinking accelerates once GCs reach the inner regions of the halo, this represents a “fine-tuning” problem. In other words, why are we observing GC3 and GC4 at such radii and not at the center if they are at a rapidly evolving stage of their decay? The same fine-tuning argument may be used against a core, however, since in that case GCs also accelerate their decay before stalling, and the timescales to sink or stall are very similar. This argument only favours a core if both clusters have stalled,

⁵ There is, of course, the possibility that these clusters are much further away in distance and lie, by chance, only in projection near the center of Fornax. This possibility may in principle be checked using the proper motions of these clusters relative to Fornax, an issue we are currently working on.

⁶ Recall that our definition of core radius follows the traditional convention of designating the distance where the density drops by a factor of two from the central value.

which requires, as discussed above, an implausibly large core radius of at least 2 kpc.

In the case of the cusp, the disadvantage of a scenario where GC3 and GC4 formed at slightly larger initial radii and are at present on their way to sinking to the center is that all clusters would then have formed outside the present-day half-light radius of the dwarf. In the absence of a well-defined theory of GC formation it is difficult to assess the severity of this objection, but it should be noted that Fornax GCs are older and more metal-poor than most stars in the dwarf. Such populations tend to be more spatially extended than younger and more metal-rich ones, in Fornax (Battaglia et al. 2006; Walker & Peñarrubia 2011) as well as in other dwarfs such as Sextans (Battaglia et al. 2011) and Sculptor (Tolstoy et al. 2004).

Some of these differences could indicate an ancient merger, which would have dispersed the old stellar component and allowed the enriched gas to sink further in before forming stars (Benítez-Llambay et al. 2016; Genina et al. 2019). This would provide a plausible explanation for the radial offset between the original distribution of Fornax GCs and the present-day distributions of its stars.

We end by noting that our simulations show no clear evidence of the “dynamical buoyancy” effects reported by Cole et al. (2012). It is thus unclear at this point what the origin of the difference might be, but it does underscore the need for further study of the effect, including a theoretical explanation and an exploration of its dependence on cluster mass and on the detailed dynamical properties of the core.

The Fornax GC spatial distribution is thus unlikely to help discern between cusp and core. In this sense, the GC timing problem is no different from dynamical analyses that use the spherical Jeans’ equations to derive mass profiles from velocity dispersion and density profile data. These models suffer from well-known degeneracies that prevent a conclusive determination of the shape of the inner density profile (see; e.g., the reviews by Strigari 2013; Walker 2013, and references therein). Indeed, data for several dSphs are consistent with NFW cusps *and* cores (e.g., Gilmore et al. 2007; Strigari et al. 2010).

Using higher-order moments of the line-of-sight velocity distribution offers in some cases the possibility of breaking the degeneracy. Recently, Read et al. (2019) applied this method to Fornax and concluded that the dark matter density drops by about an order of magnitude (from $\sim 10^8$ to $10^7 M_{\odot}/\text{kpc}^3$) over the range 0.1 to 1 kpc (see the middle panel of their Fig. 3). This is close to what is expected for a $\rho \propto r^{-1}$ NFW cusp and is only slightly less concentrated than the model we analyze here (see the middle panel of Fig. 1).

Our overall conclusion is that it is unclear how or whether the spatial distribution of GCs in Fornax may be used to discern between the core and cusp scenarios. What is clear, though, is that it cannot be used to argue convincingly against the presence of a cusp in the inner density profile of the Fornax dwarf spheroidal.

ACKNOWLEDGEMENTS

JFN acknowledges useful discussions with Justin Read.

REFERENCES

- Amorisco N. C., Agnello A., Evans N. W., 2013, *MNRAS*, **429**, L89
- Angus G. W., Diaferio A., 2009, *MNRAS*, **396**, 887
- Battaglia G., et al., 2006, *A&A*, **459**, 423
- Battaglia G., Tolstoy E., Helmi A., Irwin M., Parisi P., Hill V., Jablonka P., 2011, *MNRAS*, **411**, 1013
- Benítez-Llambay A., Navarro J. F., Abadi M. G., Gottlöber S., Yepes G., Hoffman Y., Steinmetz M., 2016, *MNRAS*, **456**, 1185
- Binney J., Tremaine S., 1987, Galactic dynamics
- Boldrini P., Mohayaee R., Silk J., 2019, *MNRAS*, **485**, 2546
- Chandrasekhar S., 1943, *ApJ*, **97**, 255
- Cole D. R., Dehnen W., Read J. I., Wilkinson M. I., 2012, *MNRAS*, **426**, 601
- Di Cintio A., Brook C. B., Macciò A. V., Stinson G. S., Knebe A., Dutton A. A., Wadsley J., 2014, *MNRAS*, **437**, 415
- Elbert O. D., Bullock J. S., Garrison-Kimmel S., Rocha M., Oñorbe J., Peter A. H. G., 2015, *MNRAS*, **453**, 29
- Fattahi A., Navarro J. F., Sawala T., Frenk C. S., Sales L. V., Oman K., Schaller M., Wang J., 2016, arXiv e-prints, p. [arXiv:1607.06479](https://arxiv.org/abs/1607.06479)
- Genina A., Frenk C. S., Benítez-Llambay A. r., Cole S., Navarro J. F., Oman K. A., Fattahi A., 2019, *MNRAS*, **488**, 2312
- Gilmore G., Wilkinson M. I., Wyse R. F. G., Kleyna J. T., Koch A., Evans N. W., Grebel E. K., 2007, *ApJ*, **663**, 948
- Goerdt T., Moore B., Read J. I., Stadel J., Zemp M., 2006, *MNRAS*, **368**, 1073
- Goerdt T., Moore B., Read J. I., Stadel J., 2010, *ApJ*, **725**, 1707
- Hernandez X., Gilmore G., 1998, *MNRAS*, **297**, 517
- Inoue S., 2009, *MNRAS*, **397**, 709
- Irwin M., Hatzidimitriou D., 1995, *MNRAS*, **277**, 1354
- Kaplinghat M., Tulin S., Yu H.-B., 2016, *Phys. Rev. Lett.*, **116**, 041302
- Kaur K., Sridhar S., 2018, *ApJ*, **868**, 134
- Ludlow A. D., Bose S., Angulo R. E., Wang L., Hellwing W. A., Navarro J. F., Cole S., Frenk C. S., 2016, *MNRAS*, **460**, 1214
- Mackey A. D., Gilmore G. F., 2003, *MNRAS*, **340**, 175
- Navarro J. F., Eke V. R., Frenk C. S., 1996a, *MNRAS*, **283**, L72
- Navarro J. F., Frenk C. S., White S. D. M., 1996b, *ApJ*, **462**, 563
- Navarro J. F., Frenk C. S., White S. D. M., 1997, *ApJ*, **490**, 493
- Oh K. S., Lin D. N. C., Richer H. B., 2000, *ApJ*, **531**, 727
- Oman K. A., Navarro J. F., Sales L. V., Fattahi A., Frenk C. S., Sawala T., Schaller M., White S. D. M., 2016, *MNRAS*, **460**, 3610
- Petts J. A., Gualandris A., Read J. I., 2015, *MNRAS*, **454**, 3778
- Pontzen A., Governato F., 2012, *MNRAS*, **421**, 3464
- Pontzen A., Governato F., 2014, *Nature*, **506**, 171
- Read J. I., Goerdt T., Moore B., Pontzen A. P., Stadel J., Lake G., 2006, *MNRAS*, **373**, 1451
- Read J. I., Walker M. G., Steger P., 2019, *MNRAS*, **484**, 1401
- Rocha M., Peter A. H. G., Bullock J. S., Kaplinghat M., Garrison-Kimmel S., Oñorbe J., Moustakas L. A., 2013, *MNRAS*, **430**, 81
- Sameie O., Yu H.-B., Sales L. V., Vogelsberger M., Zavala J., 2019, arXiv e-prints, p. [arXiv:1904.07872](https://arxiv.org/abs/1904.07872)
- Spergel D. N., Steinhardt P. J., 2000, *Phys. Rev. Lett.*, **84**, 3760
- Springel V., 2005, *MNRAS*, **364**, 1105
- Strigari L. E., 2013, *Phys. Rep.*, **531**, 1
- Strigari L. E., Frenk C. S., White S. D. M., 2010, *MNRAS*, **408**, 2364
- Tolstoy E., et al., 2004, *ApJ*, **617**, L119
- Tremaine S. D., 1976, *ApJ*, **203**, 345
- Walker M., 2013, Dark Matter in the Galactic Dwarf Spheroidal Satellites. p. 1039, [doi:10.1007/978-94-007-5612-0_20](https://doi.org/10.1007/978-94-007-5612-0_20)
- Walker M. G., Peñarrubia J., 2011, *ApJ*, **742**, 20
- Walker M. G., Mateo M., Olszewski E. W., 2009, *AJ*, **137**, 3100
- Wolf J., Martinez G. D., Bullock J. S., Kaplinghat M., Geha M., Muñoz R. R., Simon J. D., Avedo F. F., 2010, *MNRAS*, **406**, 1220